Available online at www.sciencedirect.com
SCIENCE DIRECT
Cement and Concrete Research 35 (2005) 918–925
Cement and Concrete Research

Development of a shrinkage performance specifications and prediction model analysis for supplemental cementitious material concrete mixtures

David W. Mokarem[a,*], Richard E. Weyers[b,1], D. Stephen Lane[a,2]

[a]Virginia Transportation Research Council, 530 Edgemont Road, Charlottesville, VA 22903, United States
[b]Department of Civil and Environmental Engineering, Virginia Polytechnic Institute and State University, 208 Patton Hall, Blacksburg, VA 24061-0105, United States

Received 10 October 2003; accepted 10 September 2004

Abstract

The unrestrained shrinkage along with restrained cracking tendency of concrete mixtures typically used by the Virginia Department of Transportation (VDOT) were assessed to establish an appropriate limit on drying shrinkage for use in a performance specification. Five existing shrinkage prediction models were assessed to determine the accuracy and precision of each model as it pertains to the VDOT mixtures used in this study. The five models assessed were the ACI 209 Code Model, Bazant B3 Model, CEB90 Code Model, Gardner/Lockman Model, and the Sakata Model. The Gardner/Lockman Model performed best for the supplemental cementitious material (SCM) mixtures.

Based on a comparison of the unrestrained drying shrinkage and restrained cracking tendency, it was determined that the potential for cracking could be minimized by limiting the unrestrained shrinkage of the concrete mixtures. The recommended percentage length change specification limits for the supplemental cementitious material mixtures are 0.0400 at 28 days and 0.0500 at 90 days.

Keywords: Drying shrinkage; Shrinkage prediction model; Performance specification

1. Introduction

One of the causes that result in the early deterioration of reinforced concrete involves volume changes in concrete due to autogenous shrinkage and moisture loss. As concrete cures and dries, tensile stresses are created due to hydration and loss of moisture. Drying shrinkage is defined as the decrease in concrete volume with time due to moisture loss, whereas, autogenous shrinkage is defined as the reduction in volume of the concrete due to hydration of the cement. Drying shrinkage cracking is related not only to the amount of shrinkage but also to the modulus of elasticity, creep, and tensile strength of the concrete [1].

In the case of reinforced concrete, the cracking of the concrete due to the combination of drying and autogenous shrinkage may accelerate the deterioration rate of steel reinforced concrete structures. For example, chloride ions, which are present in seawater and deicer salts, reach the concrete–steel surface either by diffusion through the water in the cracks or by capillary action. Once the chloride ions reach the steel surface, the steel will corrode, resulting in cracking, delamination, and spalling of the cover concrete.

Current research stresses the development of a low permeable concrete to reduce the effects of corrosion and other deterioration mechanisms. However, little research has been directed towards the reduction of cracking in concrete. The development of low-permeable concrete with a reduced propensity for cracking would help to reduce the deterio-

* Corresponding author. Tel.: +1 434 293 1919; fax: +1 434 293 1990.
E-mail addresses: David.Mokarem@VirginiaDOT.org (D.W. Mokarem), rweyers@vt.edu (R.E. Weyers), Stephen.Lane@VirginiaDOT.org (D.S. Lane).
[1] Tel.: +1 540 231 7408; fax: +1 540 231 7532.
[2] Tel.: +1 434 293 1953; fax: +1 434 293 1990.

0008-8846/$ - see front matter © 2004 Elsevier Ltd. All rights reserved.
doi:10.1016/j.cemconres.2004.09.013

ration of reinforced concrete from the ingress of aggressive ions and other deterioration mechanisms.

There are four main types of shrinkage in concrete: plastic shrinkage, carbonation shrinkage, autogenous shrinkage, and drying shrinkage. Plastic shrinkage is due to early age moisture loss from the concrete before, or shortly after, the concrete sets and is preventable through good construction practices. Carbonation shrinkage is caused by the chemical reaction of various cement hydration products with carbon dioxide in the air. Carbonation shrinkage is limited to the surface of the low-permeable concrete. Autogenous shrinkage is associated with the loss of water from the capillary pores due to the hydration of cement; this is commonly called self-desiccation [2]. Autogenous shrinkage tends to increase at higher temperatures and at higher cement contents. For conventional strength concrete, it is considered relatively small and is not distinguished from shrinkage caused by drying of the concrete. Drying shrinkage can be defined as the volumetric change due to the drying of concrete. This change in volume of the concrete is not equal to the volume of water lost. The loss of free water occurs first; this causes little to no shrinkage. As the drying of the concrete continues, the adsorbed water is removed. This adsorbed water is held by hydrostatic tension in the small capillaries (<50 nm). The loss of this water produces tensile stresses, which cause the concrete to shrink. The shrinkage due to this water loss is significantly larger than that associated with the loss of free water [3].

The addition of mineral and chemical admixtures can have an effect on the shrinkage of concrete. Pozzolans, such as fly ash and microsilica, and slag cement are specified in Virginia for the prevention of alkali silicate reaction and low-permeable concrete. The addition of pozzolans and slag cement generally increases the pore refinement of the concrete. This creates smaller pores and drying shrinkage is directly associated with the water held in the smaller pores. Thus, the addition of pozzolans and slag cement may increase the magnitude of drying shrinkage of the concrete.

2. Purpose and scope

The objective of the proposed study was twofold. The first objective is to develop concrete shrinkage performance specifications and an associated test procedure which may be used to limit the amount of drying shrinkage in concrete mixtures purchased by the Virginia Department of Transportation (VDOT).

The second objective was to assess the accuracy of existing unrestrained shrinkage prediction models for a range of typical VDOT mixtures.

The proposed study included A4–General Bridge Deck and A5–General Prestress concrete mixtures approved by the VDOT. Some of these mixtures included slag cement, and some included the pozzolans fly ash and microsilica. This study focused on the mixtures using supplemental cementitious materials (SCMs). Chemical admixtures such as air entrainers, retarders, and high-range water reducers were also included in the mixtures. However, they were not a study variable, as only one type and manufacturer were used.

3. Methods and materials

3.1. Restrained shrinkage testing

The restrained shrinkage testing was conducted in accordance with AASHTO PP34-98, Standard Practice for Estimating the Cracking Tendency of Concrete. The test method involves casting a concrete ring around a steel ring. Sonotube was used as a form for casting the concrete around the steel ring. Fig. 1 presents the specimen configuration. Strain gages were mounted on the inside of the steel ring to monitor the strain in the steel ring caused by the shrinkage of the concrete. As the concrete shrinks, a compressive strain is produced in the steel ring, which is balanced by a tensile strain in the concrete. When cracking occurs in the concrete, the strain and thus the stress in the steel ring is released.

The specimens were cured and measured in the following manner. Immediately after the specimens were fabricated, an initial strain measurement was conducted. Each strain gage was measured using a strain indicator. The specimens were then placed in a controlled environment of 23±2 °C and

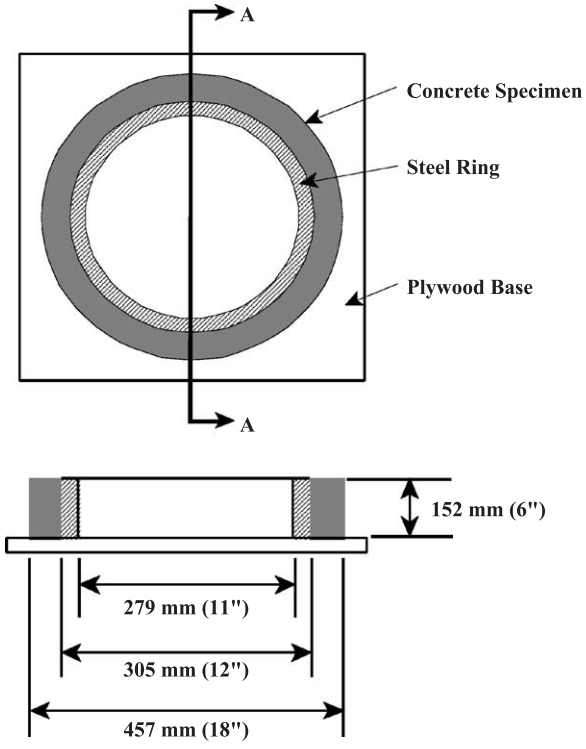

Fig. 1. Restrained shrinkage specimen configuration.

50±4% relative humidity. The specimens were covered with wet burlap and a 6-mil polyethylene sheet and allowed to cure for 24 hours. After 24 hours, the sonotube molding was removed. A 6-mil polyethylene sheet was then adhered to the top surface of the concrete ring. This was done to limit the drying of the concrete from only the annular exposed face. Strain measurements were then taken on each strain gage. Strain readings were taken again at 7 days, then every 7 days until 90 days. Subsequent readings were taken at 120, 150, and 180 days.

The specimens were visually monitored on a daily basis for cracking. Strain readings were also monitored to detect cracking. When cracking occurred, strain readings were taken on all strain gages on a daily basis for an additional 14 days. The crack width and length were also measured on a daily basis for the 14 days after cracking occurred. The crack width was measured at three locations along the crack length, and an average was calculated.

3.2. Unrestrained shrinkage testing

Unrestrained shrinkage testing was conducted in accordance with ASTM C157-98, Standard Test Method for Length Change of Hardened Hydraulic-Cement Mortar and Concrete. The test method involves measuring the length change of 75 mm × 75 mm × 279 mm concrete prisms.

Specimens were fabricated in steel molds according to ASTM C 192-98, Practice for Making and Curing Concrete Test Specimens in the Laboratory. The specimens were then covered with wet burlap and a 6-mil polyethylene sheet for 24 hours. After 24 hours of wet curing, the specimens were removed from the steel molds. Initial measurements using a comparator were then taken on each specimen in accordance with ASTM C 490-98, Practice for Use of Apparatus for the Determination of Length Change of Hardened Cement Paste, Mortar, and Concrete. After initial readings were taken, the specimens were placed in lime saturated water at 23±1 °C. The specimens were kept in the lime-saturated water for a period of 6 days, with length change measurements being conducted each day. After 6 days in lime-saturated water, the specimens were removed and placed in a controlled environment of 23±2 °C and 50±4% relative humidity. Subsequent length change measurements were conducted every 7 days up to 90 days, and then at 120, 150, and 180 days.

3.3. Compressive strength testing

Compressive strength specimens were fabricated for each concrete mixture in accordance with ASTM C 192-98. The specimens were cured in the same manner as the unrestrained shrinkage specimens. Specimens were fabricated for testing at 7, 28, 56, and 90 days. Specimens were tested in accordance with ASTM C 39-98, Test Method for Compressive Strength of Cylindrical Concrete Specimens.

3.4. Modulus of elasticity testing

Modulus of elasticity specimens were fabricated for each concrete mixture in accordance with ASTM C 192-98. Specimens were cured in the same manner as the unrestrained shrinkage specimens. Specimens were fabricated for testing at 7, 28, 56, and 90 days. Specimens were tested in accordance with ASTM C 469-98, Test Method for Static Modulus of Elasticity and Poisson's Ratio of Concrete in Compression.

3.5. Cement properties

The portland cement used in this study was a Type I/II that met ASTM C-150-98, Specification for Portland Cement. For this study, a blended Type I/II portland cement and ground granulated blast furnace slag (GGBFS) was also used for select mixtures. The GGBFS was a grade 120 and met ASTM C 989-98 Specification for Ground Granulated Blast-Furnace Slag for Use in Concrete and Mortars.

3.6. Pozzolans

The pozzolans used in this study were a Class F fly ash, and microsilica. Both pozzolans met ASTM C 311-97 specifications.

3.7. Mixture test series

Table 1 presents the mixture proportions for mixtures using supplemental cementitious materials as the binder.

The test series consisted of three A4 mixtures and one A5 mixture using diabase as the coarse aggregate. The three A4 mixtures included fly ash, microsilica, or slag cement with portland cement as the binder. The A5 mixture included slag cement and portland cement as the binder. The pozzolans and slag cement were proportioned on a weight basis in the mixtures as follows:

Fly Ash: replace 15% portland cement, replace with 20% fly ash

Table 1
Mixture proportions

Ingredient	A4-Fly ash	A4-Microsilica	A4-Slag cement	A5-Slag cement
Cement	321	351	227	252
SCM	75	27	151	167
Fine aggregate	641	669	667	670
Coarse aggregate	1138	1138	1138	1138
Water	163	163	163	164
Total	2339	2348	2346	2391
AEA (mL)	148	141	141	157
HRWR (mL)	1977	1883	1883	2090
Retarder (mL)	692	659	659	0
w/cm	.43	.43	.43	.39

Microsilica: replace 7% portland cement with 7% microsilica
Slag cement: replace 40% portland cement with 40% slag cement.

Table 2 presents the specimens fabricated for the test series.

3.8. Existing prediction models

Five existing shrinkage prediction models were used in this study to compare the actual shrinkage measurements obtained in this study to the predicted values of each model. The following presents the equations for the five existing prediction models.

3.8.1. American Concrete Institute—ACI 209 Code Model [4,5]

$$\varepsilon_{sh}\left(t,t_{sh,0}\right)=\frac{\left(t-t_{sh,0}\right)}{35+\left(t-t_{sh,0}\right)}\varepsilon_{sh\infty}\ \text{(moist/cure)}$$

$$\varepsilon_{sh}\left(t,t_{sh,0}\right)=\frac{\left(t-t_{sh,0}\right)}{55+\left(t-t_{sh,0}\right)}\varepsilon_{sh\infty}\ \text{(steam/cure)}$$

where: $\varepsilon_{sh}(t,t_{sh,0})$=shrinkage strain (in./in.); t=time (days); $t_{sh,0}$=time at start of drying (days); $\varepsilon_{sh\infty}$=ultimate shrinkage strain (in./in.).

3.8.2. Bazant B3 Model [6]

$$\varepsilon_{sh}(t,t_0)=-\varepsilon_{sh\infty}K_hS(t)$$

$$\varepsilon_{sh\infty}=-\alpha_1\alpha_2\left(26(w)^{2.1}\left(f'_c\right)^{-0.28}+270\right)10^{-6}$$

$$K_h=1-h^3$$

$$S(t)=\tanh\sqrt{\frac{t-t_0}{T_{sh}}}$$

where: $\varepsilon_{sh}(t,t_0)$=shrinkage strain (in./in.); $\varepsilon_{sh\infty}$=ultimate shrinkage strain (in./in.); α_1 and α_2=1.0; w=water content of concrete (lb/ft^3); K_h=cross-section shape factor; h=relative humidity (%); t=age of concrete (days); t_0=age of concrete at beginning of shrinkage; $S(t)$=time function for shrinkage.

Table 2
Specimen fabrication per batch

Mixture	Batches	Rings	Prisms	4×8 Cylinders	6×12 Cylinders
A4-Fly ash	3	2	6	8	1
A4-Microsilica	3	2	6	8	1
A4-Slag cement	3	2	6	8	1
A5-Slag cement	3	2	6	8	1

3.8.3. Euro-International Concrete Committee—CEB 90 Code Model [4,5]

$$\varepsilon_{cso}=\varepsilon_s(f_{cm})(\beta_{RH})$$

$$\varepsilon_S(f_{cm})=(160+10\beta_{sc}(9-f_{cm}/1450))10^{-6}$$

$$\beta_{RH}=-1.55\beta_{ARH}$$

$$\beta_{ARH}=1-(RH/100)^3$$

where: ε_{cso}=drying shrinkage of portland cement concrete (in./in.); ε_s=drying shrinkage obtained from RH-shrinkage chart; β_{sc}=coefficient depending on type of cement; β_{RH}=coefficient for relative humidity; f_{cm}=mean 28-day compressive strength (psi).

3.8.4. Gardner/Lockman Model [7]

$$\varepsilon_{sh}=\varepsilon_{shu}\beta(h)\beta(t)$$

$$\varepsilon_{shu}=1000K\left(\frac{4350}{f'_{cm28}}\right)^{1/2}10^{-6}$$

$$\beta(h)=1-1.18h^4$$

$$\beta(t)=\left(\frac{(t-t_c)}{t-t_c+97(V/S)^{1/2}}\right)10^{-6}$$

where: ε_{sh}=shrinkage strain (in./in.); ε_{shu}=ultimate shrinkage strain (in./in.); $\beta(h)$=correction term for effect of humidity on shrinkage; $\beta(t)$=correction term for effect of time on shrinkage; h=humidity; t_c=age drying commenced (days); t=age of concrete (days).

3.8.5. Sakata Model [8]

$$\varepsilon_{sh}(t,t_0)=\varepsilon_{sh\infty}\left[1-\exp\left\{-0.108(t-t_0)^{0.56}\right]\right.$$

$$\varepsilon_{sh\infty}=-50+78(1-\exp(RH/100)+38(\ln(w))-5(\ln(V/S)/10))^2\,10^{-5}$$

where: $\varepsilon_{sh}(t,t_0)$=predicted shrinkage strain (in./in.); $\varepsilon_{sh\infty}$=ultimate shrinkage strain (in./in.); w=water content of the concrete (kg/m^3); RH=relative humidity (%); V/S=volume-to-surface area ratio; t=time (days); t_0=time drying started (days).

4. Results and discussion

4.1. Compressive strength

One of the factors that contributes to the compressive strength of concrete is the water-to-cement (w/c) ratio of the

mixture. A mixture with a lower w/c ratio may produce a higher compressive strength. Table 3 presents the average compressive strengths at 7, 28, and 90 days after casting.

For the supplemental cementitious material mixtures, the A4 mixtures had a w/c ratio of 0.43 and the A5 mixture had a w/c ratio of 0.39. The A5 mixture had the highest compressive strengths. For the A4 mixtures, the mixture using slag cement had a higher compressive strength than the mixtures using fly ash and microsilica.

4.2. Modulus of elasticity

Table 4 presents the average modulus of elasticity for the mixtures performed in this study at 7, 28, and 90 days after casting of the specimens. The test was performed twice at 7, 28, and 90 days, and the modulus of elasticity values in the table represent the average of the two measurements.

For the A4 mixtures, the mixture using the slag cement had a higher average modulus of elasticity than the mixtures using the fly ash and microsilica. The A5 mixture using the slag cement had the highest average modulus of elasticity.

4.3. Unrestrained shrinkage

Table 5 presents the average percent length change for unrestrained concrete specimens at 7, 28, 56, 90, 120, 150, and 180 days. The mixtures include the supplemental cementitious material mixtures as well as A4 and A5 portland cement concrete mixtures [9].

For the supplemental cementitious material mixtures, the mixture containing the fly ash exhibited the greatest amount of shrinkage. The mixtures containing microsilica and slag cement were not significantly different. The A4 mixtures containing supplemental cementitious materials had the same w/c ratio and aggregate type, diabase.

The w/c ratios for the A4 and A5 slag cement mixtures were 0.43 and 0.39, respectively. For the slag cement mixtures, the w/c ratio did not have a significant effect on the shrinkage values.

The supplemental cementitious material mixtures exhibited greater drying shrinkage than the associated portland cement concrete mixtures. This could be due to the denser matrix produced by the fly ash, microsilica, and slag cement. This denser matrix would create smaller capillary voids, and the bulk of drying shrinkage in concrete occurs from the loss of water from the smaller capillary voids.

Table 3
Average compressive strength test results (MPa)

Mixture	7 Days	28 Days	90 Days
A4-Fly ash	47.9	53.4	58.1
A4-Microsilica	47.3	52.8	60.1
A4-Slag cement	50.2	54.3	61.0
A5-Slag cement	51.3	55.3	62.3

Table 4
Average modulus of elasticity test results (GPa)

Mixture	7 Days	28 Days	90 Days
A4-Fly ash	31.2	35.3	40.8
A4-Microsilica	30.4	35.5	42.1
A4-Slag cement	33.3	37.0	42.3
A5-Slag cement	33.1	38.1	44.6

4.4. Restrained shrinkage

Table 6 presents the average microstrain values for the restrained concrete specimens at 7, 28, 56, 90, 120, 150, and 180 days. The supplemental cementitious material microstrain is the average of 32 strain gages on eight rings. The A4 and A5 portland cement concrete mixtures are the average of 24 strain gages on six rings for each group.

None of the supplemental cementitious material rings experienced cracking. The average microstrain values ranged from −142 to −193, with the fly ash mixtures experiencing the highest strain, and the A4 slag cement mixture experiencing the least strain. The A4 and A5 slag cement mixtures had less strain than the microsilica and fly ash mixtures. It should be noted that the fly ash mixtures experienced higher shrinkage values for both the unrestrained and restrained conditions. Four of the portland cement concrete rings cracked. All four rings had an average microstrain of greater than 200 when they cracked.

4.5. Relationship between percentage length change and microstrain

As shown in Table 6, those specimens which cracked within 180 days (A4 and A5 portland cement concrete mixtures) had an average microstrain of greater than 200 microstrain, and those that did not crack had less than 200 microstrain. Therefore, it appears that if the strain produced in a restrained situation is greater than 200 με, there is an increased probability of cracking.

The percentage length change was plotted versus the microstrain for each mixture to determine if there was a correlation between them. Fig. 2 presents the percentage length change versus microstrain for the supplemental cementitious material mixtures. Note that these mixtures used the same aggregate type, diabase, and the associated fine aggregate. Moreover, the water to cement plus pozzolan ratios were the same, 0.43. For the supplemental cementitious concrete material mixtures, there is a strong correlation between the percentage length change and microstrain. Using a value of 200 με in the linear equation from Fig. 2, one would obtain a value of 0.0516 for the percentage length change. Thus, if the percentage length change is greater than 0.0516, there is an increased probability of cracking for these mixtures. Based on the results obtained from the correlation between percentage length change and microstrain, a performance specification may be developed. The above results demonstrate that if the microstrain in the

Table 5
Average percentage length change (unrestrained shrinkage specimens)

Mixture	7 Days	28 Days	56 Days	90 Days	120 Days	150 Days	180 Days
A4-Fly ash	−.0197	−.0396	−.0487	−.0522	−.0537	−.0547	−.0561
A4-Microsilica	−.0187	−.0367	−.0433	−.0447	−.0473	−.0490	−.0510
A4-Slag cement	−.0204	−.0385	−.0429	−.0474	−.0490	−.0499	−.0530
A5-Slag cement	−.0198	−.0354	−.0425	−.0457	−.0478	−.0491	−.0500
A4-PCC	−.0155	−.0250	−.0352	−.0389	−.0414	−.0432	−.0458
A5-PCC	−.0164	−.0249	−.0338	−.0381	−.0400	−.0413	−.0434

restrained shrinkage specimens is greater than 200με, at 90 days, there is an increased probability of cracking. Calculating the associated percentage length change from linear equations for each mixture group, the percentage length change is to be limited to 0.0400 at 28 days and 0.500 at 90 days for these mixtures.

4.6. Prediction models

A predicted percent unrestrained shrinkage was calculated for each of the five models at 7, 28, 56, 90, 120, 150, and 180 days after shrinkage had commenced. A residual value for each measured unrestrained shrinkage specimen was calculated as follows:

$$\text{Residual value} = \text{Predicted value} - \text{Measured (Experimental) value} \quad (1)$$

Thus, if the residual value was positive, it indicated that the model over estimated the shrinkage. If the residual value was negative, it indicated that the model underestimated the shrinkage.

The residuals are an indication of the models ability to either overestimate or underestimate shrinkage. However, the residuals do not necessarily determine which model is the best predictor. To determine which model is the best predictor, two analyses were performed: an error percentage analysis and the summation of the residuals squared test. The error percentage was calculated as follows for the residual values at 7, 28, 56, 90, 120, 150, and 180 days:

$$\text{Error percentage} = (\text{Residual value}*100)/\text{Experimental value} \quad (2)$$

The ACI 209 and Sakata models are applicable for only Type I General and Type III High Early Strength cements. Therefore, residuals were not calculated for the A4-Diabase/Fly ash, A4-Diabase/Slag cement, and A5-Diabase/Slag cement mixtures for the ACI 209 and Sakata models because these cementing materials hydrate at a slower rate than a Type I or Type III cement. For the fly ash and slag cement mixtures, the Bazant, CEB90, and Gardner/Lockman models were used in shrinkage prediction analyses because these cementing materials are closer in hydration characteristics to a Type II Cement rather than a Type I.

For the summation of the residuals, squared model with the smallest value indicates the best predictor. Table 7 presents the models average error percentages and summation of the residuals squared for the supplemental cementitious material mixtures.

The rank order of the best to worst prediction model using the error percentage for the A4 fly ash and the A4 and A5 slag cement mixtures is the Gardner/Lockman model, with the CEB90 and Bazant models being equivalents. Whereas all of the models were poor predictors for the A4 microsilica mixture. Overall, for the error percentage, analysis of the data underestimated the shrinkage of the supplemental cementitious material mixtures. For the supplemental cementitious material mixtures, the Gardner/Lockman model was the best predictor. It was consistently better than the Bazant and CEB90 models for the mixtures that were considered to be type II cement.

For the summation of the residuals squared fly ash mixtures, the Gardner/Lockman model was the best predictor followed by the Bazant and CEB90 models. The values for the A4 slag cement mixture demonstrate that the Gardner/Lockman model is the best predictor, followed by the Bazant and CEB90 models. The same is true of the A5 slag cement mixtures.

For the microsilica mixture, considered to be type I cement mixtures, the summation of the residuals squared

Table 6
Average microstrain (restrained shrinkage specimens)

Mixture	7 Days	28 Days	56 Days	90 Days	120 Days	150 Days	180 Days
A4-Fly ash	−60	−119	−136	−178	−184	−188	−193
A4-Microsilica	−61	−93	−106	−141	−154	−163	−172
A4-Slag cement	−52	−83	−96	−125	−129	−136	−142
A5-Slag cement	−57	−103	−114	−125	−137	−148	−157
A4-PCC	−53	−93	−140	−171	−177	−182	−215
A5-PCC	−57	−88	−122	−162	−172	−183	−220

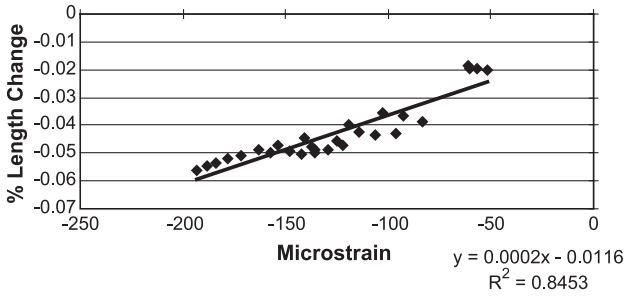

Fig. 2. Percentage length change vs. microstrain for SCM mixtures.

values demonstrated that the ACI 209 model is the best predictor. The Bazant and CEB90 models followed closely. The Gardner/Lockman model was the fourth best predictor. The ACI 209 and Sakata models overestimated the shrinkage, while the Bazant, CEB90, and Gardner/Lockman models underestimated the shrinkage. The same analysis was performed assuming that the mixtures were a type II cement. In this case, the Gardner/Lockman model was the best predictor. The reason for the skewed results using a type I cement analysis is that the actual measured shrinkage values were high, and the models are strongly based on compressive strength. The models assume that a higher 28-day compressive strength will have less shrinkage; however, this may not be true for all cases.

4.7. Summary of error percentage and summation of residuals squared analysis

The error percentage and the summation of the residuals squared analyses demonstrated the same results in terms of the model performance from best to worst. As mentioned previously, the models predict shrinkage largely based on the 28-day compressive strength of a mixture. A lower compressive strength results in a higher predicted shrinkage for these models. The compressive strength parameter is used in an effort to account for the effects of water and cement; a lower w/c ratio should indicate a lower water content, thus less shrinkage. Although compressive strength influences the amount of shrinkage, there are other factors that need to be considered. These factors include the pore volume and pore size distribution. The majority of drying shrinkage is associated with the loss of water from the smaller capillary voids in the concrete. A concrete mixture using supplemental cementitious materials such as fly ash, microsilica, and slag cement have a more refined pore structure than ordinary portland cement concrete mixtures. There are more smaller capillary voids in these mixtures and the removal of water from these voids may result in more drying shrinkage.

5. Conclusions

- The mixtures containing fly ash exhibited greater drying shrinkage than those containing microsilica and slag cement.
- There is a correlation between the percentage length change for unrestrained shrinkage specimens and microstrain for restrained shrinkage specimens. Thus, the unrestrained shrinkage test may be used as a performance based specification for restrained concrete systems.
- Based on the results of this study, the percentage length change for the supplemental cementitious material mixtures should be limited to 0.0400 at 28 days and 0.0500 at 90 days to reduce the probability of cracking due to drying shrinkage.
- The Gardner/Lockman model is the best predictor of drying shrinkage for the fly ash and slag cement mixtures followed by the Bazant B3, and CEB90 models.

Acknowledgements

This research was supported by the Virginia Transportation Research Council; their financial support is gratefully acknowledged. The findings, opinions, and conclusions are those of the authors and not necessarily those of the sponsoring agency.

Table 7
Summary of error percentage and sum of residuals squared analysis

Model		A4-Fly ash	A4-Microsilica	A4-Slag cement	A5-Slag cement
ACI 209	Error %	–	110	–	–
	Σ Resid.^{2}	–	917183	–	–
Bazant	Error %	30	78	24	22
	Σ Resid.^{2}	2091265	1025177	1183138	1005714
CEB 90	Error %	30	78	25	24
	Σ Resid.^{2}	2291212	1116906	1393315	1304490
Gardner/Lockman	Error %	20	67	14	13
	Σ Resid.^{2}	1104398	2198880	505403	451229
Sakata	Error %	–	145	–	–
	Σ Resid.^{2}	–	4367955	–	–

References

[1] P.K. Mehta, P.J.M. Monteiro, Concrete Structure, Properties, and Materials, Prentice Hall, New Jersey, 1993.
[2] D. Carlton, P.J.M. Mistry, Thermo-elastic-creep analysis of maturing concrete, Comput. Struct. 40 (2) (1991) 293–302.
[3] A.M. Neville, Properties of Concrete, John Wiley & Sons, New York, 1998.
[4] N.S. Bhal, M.K. Mital, Effect of relative humidity on creep and shrinkage of concrete, Indian Concr. J. 70 (1) (1996 January) 21–27.
[5] P.K. Mehta, P.J.M. Monteiro, Concrete Structure, Properties, and Materials, Prentice Hall, New Jersey, 1986.
[6] Z.P. Bazant, Creep and shrinkage prediction model for analysis and design of concrete structures—model B3, Mat. Struct. 28 (1995) 357–365.
[7] N.J. Gardner, M.J. Lockman, Design provisions for drying shrinkage and creep of normal-strength concrete, ACI Mater. J. 98 (2001) 159–167.
[8] K. Sakata, Prediction of concrete creep and shrinkage, creep and shrinkage of concrete, Proceedings of the Fifth International RILEM Symposium, Barcelona, Spain, September 6–9, 1993, pp. 649–654.
[9] Mokarem, D.W., Development of Concrete Shrinkage Performance Specifications, Ph.D. dissertation, Virginia Polytechnic Institute and State University, May 2002.